Resources, Conservation & Recycling Advances 25 (2025) 200244

Contents lists available at ScienceDirect

Resources, Conservation & Recycling Advances

journal homepage: www.sciencedirect.com/journal/Resources-Conservation-and-Recycling-Advances

Upcycling of medium-density fiberboard and polyurethane foam wastes into novel composite materials

Aleksander Hejna [a,*], Mateusz Barczewski [a], Joanna Aniśko [a], Adam Piasecki [b], Roman Barczewski [c], Paulina Kosmela [d], Jacek Andrzejewski [a], Marek Szostak [a]

[a] Institute of Materials Technology, Poznan University of Technology, 61-138 Poznań, Poland
[b] Institute of Materials Engineering, Poznan University of Technology, 60-965 Poznań, Poland
[c] Institute of Applied Mechanics, Poznan University of Technology, 60-965 Poznań, Poland
[d] Department of Polymer Technology, Gdańsk University of Technology, 80-233 Gdańsk, Poland

ARTICLE INFO

Keywords:
Bulky wastes
Polyurethane foams
Medium-density fiberboards
Waste management
Composites
Binder

ABSTRACT

While plastic and e-waste dominate public discourse, municipal waste, particularly bulky wastes pose a significant challenge due to their large-scale generation aligning with the enrichment of society. Their efficient collection and keeping in a loop should be considered among the priorities of municipal waste management. Herein, the presented work presents novel composite materials obtained from flexible polyurethane foams used as mattresses and medium-density fiberboards applied in furniture products. Composites have been prepared using compression molding, with the addition of an innovative binder composed of a diisocyanate and inorganic salt, whose in situ decomposition led to the gas generation providing the porous structure and strengthening the interfacial bonding inside the material. The impact of changes induced by the chemical interactions on the appearance, morphology, mechanical, thermal, acoustic and insulation performance of composites has been evaluated. Observed changes pointed to the auspicious conclusions on the further applications of the examined binder composition.

1. Introduction

Significant environmental pollution from anthropogenic waste, affecting almost every area of the planet and affecting every aspect of human life, has significantly contributed to the development of the concept of a Circular Economy, the introduction of which implies a significant reduction in the adverse impact of human activity on the environment (Payne et al., 2019; Zhao et al., 2022). The move toward circularity is driven by changing human perception and bottom-up created pro-environmental sustainability trends, which over time have resulted in the development of local, national, international, and even global regulations, such as, among others, the Kyoto Protocol, which aims to aims to reduce greenhouse gas emissions (Bohringer, 2003). In recent years, the European Union (EU), through directives and climate targets, has obliged member countries to orient industry toward secondary and renewable raw materials. In 2019, the European Green Deal was presented as a map for achieving a sustainable economy (European Comission, 2019). In 2020, the EU presented "A new Circular Economy Action Plan For a cleaner and more competitive Europe", as well as the 2030 Climate Target Plan (European Comission, 2020a, 2020b). One of their main goals is to reduce greenhouse gas emissions (by at least 55 % by 2030 compared to 1990). Nowadays, the pursuit of circularity is therefore essential not only for environmental reasons but increasingly for economic reasons, which is related to the targets set by the EU for the prevention of waste generation and its recycling and the penalties threatening for not meeting the requirements (European Environment Agency, 2023).

Currently, in addition to plastic waste, electronic waste, or batteries, a robust emphasis is being placed on the efficient management of municipal waste, which, according to Statistics Poland, people are producing more and more. In 2022, Poles generated 13.4 million tons of municipal waste, an increase of as much as 2.8 million tons compared to 2015 (Glowny Urzad Statystyczny, 2023). It is essential to collect them separately (currently about 40 %), which improves and reduces the cost of their management by energy recovery or recycling. One of the groups of municipal waste is bulky waste, i.e., waste that does not fit into commonly used garbage containers. This mainly includes furniture, upholstered goods, carpets, rugs, bicycles, or baby carriages. The first

* Corresponding author.
E-mail address: aleksander.hejna@put.poznan.pl (A. Hejna).

https://doi.org/10.1016/j.rcradv.2025.200244

Available online 9 January 2025

two groups dominate among them, which is related to the dynamic situation in the real estate market, including rentals and, consequently, the renovation and refurbishment of apartments. Media reports suggest a decrease in bulky waste due to the economic situation, which, however, is contradicted by the Statistics Poland data presented in the above-cited report. The inaccuracies may be related to the growing popularity of social movements related to the provision of information on bulky waste in the days before the relevant services collect them. This is related to the growing environmental awareness of the society, which is expressed by going beyond the principle that has been known for years as 3R - Reduce, Reuse, Recycle and moving closer to the now postulated 9R Principle - Refuse, Rethink, Reduce, Reuse, Repair, Refurbish, Remanufacture, Repurpose, Recycle, Recovery (Kirchherr et al., 2017). All of these activities are aimed at extending the life of products and their parts, which represents a further step from a linear economy to a Circular Economy in relation to processes involving the efficient use of materials (from which products are made), such as recycling or energy recovery. According to the 9R Principle, the activities closest to circularity are those concerning smarter use and manufacturing of products, i.e., refuse, rethink, and reduce (de Melo et al., 2022; Muñoz et al., 2024). In the case of bulky waste, the ideal solution seems to be to reject or rethink the use of the original products, which would result in a reduction in the amount of waste generated, but achieving this state requires further, also far-reaching changes in public awareness induced by appropriate education.

In the current situation, a favorable alternative, allowing to achieve both financial and environmental benefits, is to recycle bulky waste and use it in further production processes production in order to reduce the consumption of primary and natural resources, which qualifies as a smarter use and products manufacturing. When recycling bulky waste, it is essential to recover wood, as it is estimated that each ton of wood recovered reduces the CO_2 emissions into the atmosphere by as much as two tons and reduces the need to cut down healthy trees (Lauri et al., 2012). On the other hand, wood-based materials, containing the addition of various types of binders, binders, or impregnates, which are also an essential part of bulky waste, are most often burned in dedicated installations for this purpose and used as a raw material for energy, which is the lowest level of circularity (Ding et al., 2023). Therefore, it is imperative to look for opportunities for further use of this type of waste, enabling them to be kept in a loop, which will be an essential step towards the Circular Economy.

The presented study aimed to investigate the possibility of producing novel composite materials with potential use in the construction and building sector from bulky wastes, particularly medium-density fiberboards (MDFs) and polyurethane foams (PUFs) from post-consumer furniture products. Simultaneous application of these materials could not only yield an efficient management approach for furniture wastes but also provide auspicious features for the final composites resulting from the specific properties of particular components. The low apparent density of PUFs yields materials with reduced density and thus leads to a reduction in the share of adhesive resins, which are primarily responsible for the volatile organic compound emissions from engineered wood material (Boruszewski et al., 2022). Reduced density and the presence of pores inside the structure may enhance thermal insulation performance, as reported by Hýsek et al. (2019), who applied recycled polyurethane (PU) mattress foam to produce insulation panels with wheat husks. Mao et al. (2014) pointed to the serior mechanical performance of particleboards in which polymeric isocyanate binder was partially substituted with micronized PUF powders.

In the presented case, multiple composite particleboards with varying contents of MDF and PUF wastes have been prepared by compression molding technology with the application of an innovative binder composed of diisocyanate and inorganic salt, whose in situ decomposition led to the gas generation providing porous structure of final composites, and produced compounds strengthening the interfacial bonding inside the material. Moreover, the application of the binder composition can reduce the use of methylene diphenyl diisocyanate, which, despite its popularity in the manufacturing of engineered wood materials, is considered toxic and harmful. The impact of applied formulations and manufacturing procedures on the structure, mechanical, thermal, insulation, and acoustic performance of resulting composites have been explored. The presented results indicated that proper engineering of materials' composition and preparation could find a compromise between the weight, mechanical performance, and other functionalities required by the particular applications.

2. Experimental

2.1. Materials

The following study has applied two types of materials originating from bulky wastes: flexible PUFs and waste MDF. PUFs were obtained using a single-step method on a laboratory scale from commercially available and widely applied in industry PU system, comprising of SPECFLEX® NF 706 polyol and SPECFLEX® NE 434 isocyanate, acquired from MB Market (Poland). Foams were prepared using a closed aluminum mold, similar to those applied in the manufacturing of, e.g., automotive or train seats. Properties of used foams were as follows: apparent density of 185 ± 5 kg/m^3, open cell content of 60 ± 3 %, thermal conductivity coefficient of 66 ± 2 mW/(m·K), and tensile strength of 150 ± 13 kPa. Prior to the preparation of composite materials, waste PUFs were ground using a two-roll mill and passed through a 2.8 mm sieve. MDF wastes were obtained from the local company (Poland). Fig. S1 provides information on the particle size distribution and images of particular fractions obtained using optical microscopy.

Moreover, during manufacturing, the 4,4′-methylene diphenyl diisocyanate (MDI) and ammonium bicarbonate (AB), both obtained from Sigma-Aldrich (Poland) and applied as received, were used as binders for composite materials following our patent application (Hejna and Barczewski, 2024).

2.2. Preparation of composite materials

Previously calculated amounts of PUFs, MDF, MDI, and AB, were placed in a planetary mixer Gerlach GL 4219 (Germany) and mixed for 3 min. Mixing time was adjusted based on our previous yet unpublished work. The proper amount of mixture was then placed in a metal mold and compression molded using a Fontjine LabManual 300 (Netherlands) laboratory hydraulic press. Table 1 provides details on applied formulations and compression molding parameters.

The application of MDI and AB as binder components was based on their chemical interactions with PUF and MDF wastes, which are presented in Fig. 1. The application of diisocyanates as binders in recycled PU or engineered wood materials has been repeatedly reported in the literature (Ding et al., 2023; Ma et al., 2022; Zia et al., 2007) and was the basis for our study. Nevertheless, there are numerous concerns about using diisocyanates related to their toxicity and reactivity (Khatoon et al., 2021; Niesiobędzka and Datta, 2023). One of the goals of the presented study was to reduce its content in developed composites by introducing AB. The incorporation of AB was also aimed at enhancing the decomposition of the PUF phase during processing, simultaneously strengthening interfacial interactions with MDF particles and providing additional crosslinking, as indicated by the presented chemical reactions. Fig. S2 presents the results of thermogravimetric analysis (TGA) of applied PUF and AB, which confirm the occurrence of the mentioned decomposition reactions in the analyzed temperature range.

Reactions (a) and (b) are related to the two main decomposition mechanisms of urethane groups occurring in the applied temperature range; hence, the dissociation of the urethane bond and formation of primary amine with simultaneous carbon dioxide release (Levchik and Weil, 2004). Based on the presented TGA results, these reactions occur in the range of 145–250 °C. However, elongated residence time in mold

Table 1
Formulations applied during the manufacturing of composite samples via compression molding.

Sample	Content, wt%			Binder composition, MDI:AB molar ratio	Molding temperature, C	Molding time, min
	PUF	MDF	Binder			
1	90	0	10	1:0	160	5
2	67.5	22.5	10	1:0	160	5
3	45	45	10	1:0	160	5
4	22.5	67.5	10	1:0	160	5
5	47.5	47.5	5	1:0	160	5
6	42.5	42.5	15	1:0	160	5
7	45	45	10	3:1	160	5
8	45	45	10	2:1	160	5
9	45	45	10	1:1	160	5
10	45	45	10	1:2	160	5
11	45	45	10	1:3	160	5
12	45	45	10	1:1	120	5
13	45	45	10	1:1	140	5
14	45	45	10	1:1	180	5
15	45	45	10	1:1	200	5
16	45	45	10	1:1	160	1
17	45	45	10	1:1	160	2.5
18	45	45	10	1:1	160	10
19	45	45	10	1:1	160	15

and applied pressure may accelerate the decomposition (Allan et al., 2019). Reaction (c) indicates the mechanism of AB thermal decomposition, occurring in the range of 45–130 °C, as suggested by performed TGA analysis (Fig. S2). Notably, the basic character of ammonia may catalyze the decomposition of urethane groups and shift the degradation range toward lower temperatures (Gu et al., 2023). Reactions (d)-(f) present the chemical reactions between MDI and PUFs' decomposition products, leading to the formation of allophanate, urethane, and urea groups, which may contribute to the crosslinking inside developed composites. Moreover, reaction (e) can also include hydroxyl groups present in the wood particles of MDF waste, therefore leading to interfacial adhesion strengthening. Reactions (g) and (h) can occur between MDI and AB, two components of the applied binder. Finally, reactions (i) and (j) may additionally contribute to interfacial crosslinking by the generation of biuret moieties. Notably, to enhance clarity, the reaction schemes presented above include only one free isocyanate group. However, the MDI applied as a binder in the developed material contains two isocyanate groups, which are characterized by the same reactivity, which significantly enhances the interfacial crosslinking.

Considering the literature data on the reactivity of isocyanate groups with particular active hydrogen compounds (Vilar, 1998), reactions with ammonia or primary amines occur at the highest rates (relative reaction rate of 100 000), followed by the reactions with primary hydroxyls and water (100), secondary hydroxyls (30), ureas (15), and urethanes (0.3). These reaction rates are characteristic of uncatalyzed reactions occurring at 25 °C, but they may provide insights into potential interactions during the development of presented composites. Based on the reaction schemes and rates, urea groups should be the most abundant in the developed materials.

2.3. Characterization techniques

Fourier transform infrared spectroscopy (FTIR) was performed using the Jasco (Japan) FT/IR-4600 apparatus equipped for working in attenuated total reflectance (ATR) mode. FTIR analyses were carried out using 64 scans at a resolution of 4 cm^{-1} in the wavenumber range of 4000–400 cm^{-1}.

The samples' morphology was evaluated using a digital microscope, Keyence VHX 7000 (Belgium), and a scanning electron microscope (SEM), Tescan MIRA3 (Czech Republic). For the SEM, a thin carbon coating with a thickness of approximately 20 nm was deposited on samples using a Jeol JEE 4B vacuum evaporator (Japan). The cellular structures of foams were analyzed using an accelerating voltage of 5 kV. The secondary electron detector was used.

The thermal conductivity coefficient (λ) of prepared polyurethane foams was determined using the heat flow meter HFM 446 from Netzsch (Germany). Samples with a thickness of 4 mm were tested in the

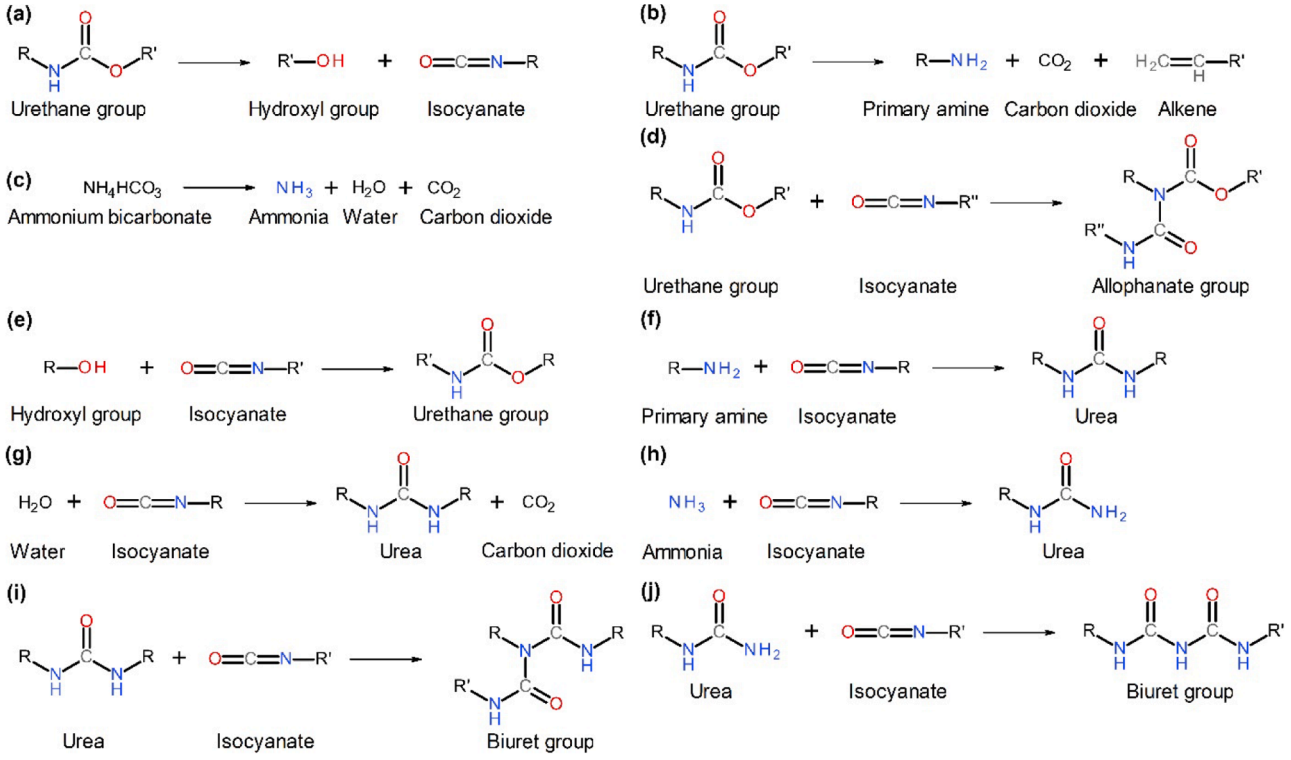

Fig. 1. The chemical reactions potentially occurring between the particular components of prepared composites.

temperature range from 20 to 35, 40, 45 or 50 °C using the average temperature of 27.5, 30.0, 32.5 or 35.0 °C.

The Shore hardness type 0 of prepared composites was evaluated with Sauter HB0 100-0 durometer (Germany) following ASTM 2240 standard. At least 15 measurements were performed for each of the tested series.

The flexural strength of composites was measured following ASTM D790. The beam-shaped samples with 4 × 10 × 100 mm^3 dimensions were measured with a slide caliper with an accuracy of 0.1 mm. The bending test was performed using Zwick/Roell Z020 model 5101 universal testing machine (Germany) at 25 °C and relative humidity of 30 % at a 10 mm/min constant speed. The presented data is the average value of at least seven measurements for static flexural experiments.

The thermogravimetric (TGA) analysis of composites was performed using the TG 209 F3 apparatus from Netzsch (Germany). Samples weighing approximately 10 mg were placed in a ceramic dish. The study was conducted in a nitrogen atmosphere at 25–900 °C with a heating rate of 10 °C/min.

The determination of the sound absorption coefficients of novel materials was carried out following the ISO 10534-2 and ASTM E1050-8 standards. The following equipment was used to carry out the tests: two BSWA impedance tubes (SW422 and SW 744), MC 3242 data acquisition hardware, PA50 power amplifier, BSWA VA LAB4 software (China), and two Roga Instruments MI 19 microphones - ¼ inch IEPE standard (Germany). The measuring system was calibrated with a CA114 acoustic calibrator from BSWA Technologies Co. Ltd. (China). Atmospheric pressure, temperature, and air humidity were monitored with the LAB-EL LB-575 climate meter (Poland). To cover the 100–6300 Hz range, two types of samples in the form of discs with 30 and 100 mm diameter were cut from the manufactured samples. The test results are presented as characteristics containing the values of sound absorption coefficients in 1/3 octave bands (100–6300 Hz). The characteristics were created based on partial results obtained in the bands 63–500 Hz and 250–1600 Hz (using an impedance tube with a diameter of 100 mm and different spacing of microphones) and in the band 1000–6300 Hz (using a tube SW744 with a diameter of 30 mm). The final result for each sample is the result of averaging three measurements.

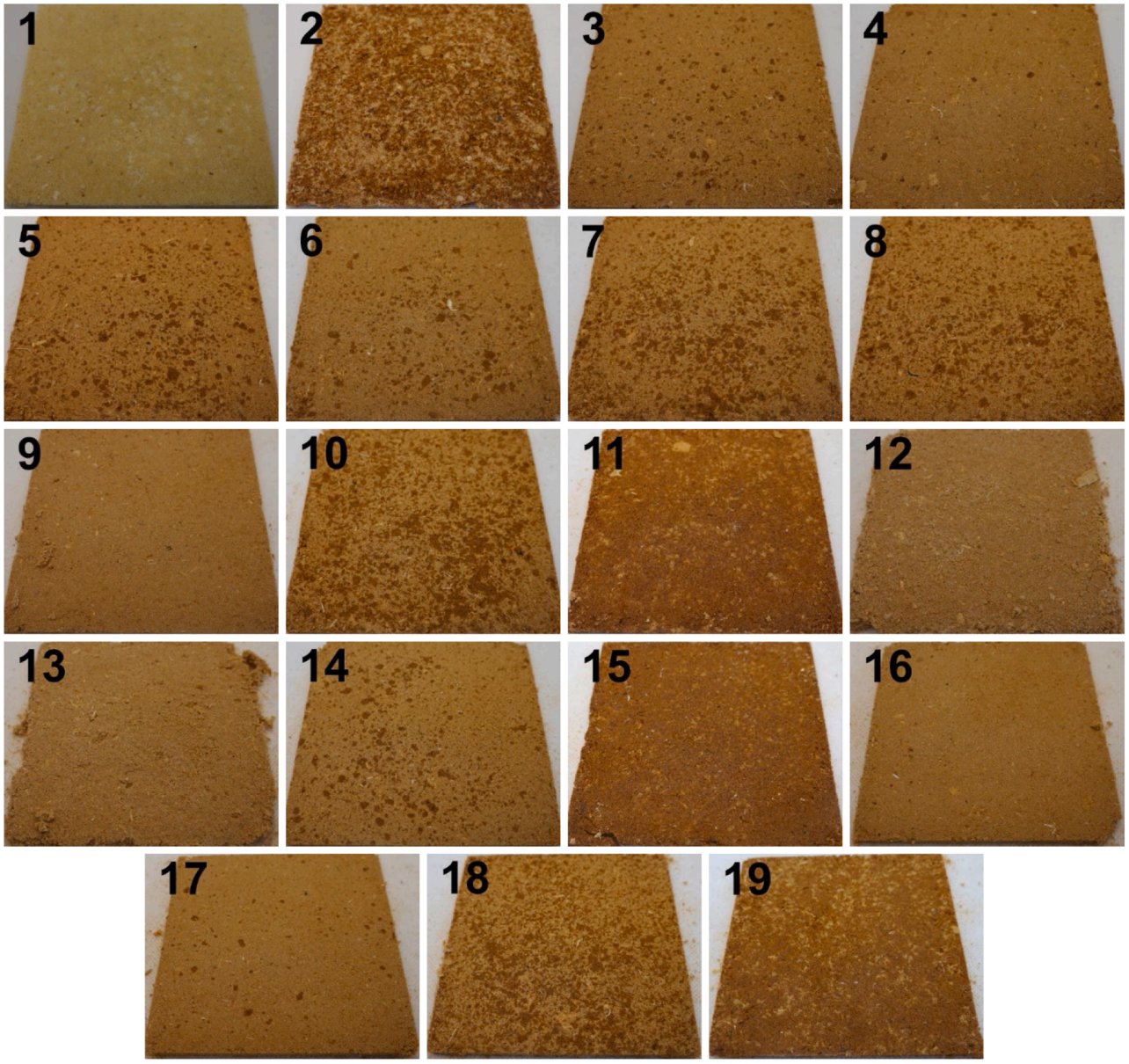

Fig. 2. The appearance of prepared composite materials.

3. Results and discussion

3.1. Visual assessment of prepared composites

Fig. 2 presents the appearance of prepared composites, which significantly varied between applied formulations, especially the contents of PUF and MDF wastes (samples 1–4), the content of binder (samples 3, 5, and 6), the composition of binder (samples 7–11), compression molding temperature (samples 9 and 12–15), and time (samples 9 and 16–19).

Based on the appearance of samples and results further described, equal contents of PUF and MDF wastes have been applied for further tests. Application of 22.5 wt% of PUF wastes (sample 4) yielded high brittleness of composites resulting in defragmentation and fracturing during demolding step. On the other hand, using 67.5 wt% of PUF wastes (sample 2) made the surface sticky due to thermally induced decomposition, which could be very beneficial when thermally decomposed PUF wastes would be applied as an adhesive layer for oriented strand boards or veneers, but not in the presented case.

Accordingly, the molding parameters, temperature, and time were selected. Too low temperatures of 120 and 140 °C (samples 12 and 13), as well as short processing times (samples 16 and 17), yielded fragile structures and fractures during demolding. On the other hand, the application of 200 °C (sample 15) or 15 min of compression molding (sample 19) caused surplus PUF decomposition, which, again, could be very desirable for different applications. Therefore, for further tests, a compression molding temperature of 160 °C and a time of 5 min were selected.

Too high brittleness has also been noted for the 5 wt% content of the binder, while 15 wt% did not yield significant differences from 10 wt%. Considering binder composition, the MDI was combined with AB due to the potential chemical interactions at elevated temperatures described above. The incorporation of AB provided a beneficial impact on the composites' structure, yielding better packing of material (infill degree of the molding cavity) and reduced amount of macroscopic pores and voids. At the same time, a significant excess of AB caused excessive degradation of the PUF phase and limited the performance of composites in developed form. Such an effect could be associated with the low particle size of applied MDF wastes.

3.2. Chemical structure of prepared composites

Fig. 3 presents the FTIR spectra of the particular composite samples, pointing to the differences in their chemical structure and the additional plot showing the variations in the intensity of the 1090 cm^{-1} peak attributed to the vibrations of C═O bonds in urethane groups. Clearly, the most significant variations have been observed for changing PU:MDF ratio, which can be associated with the different chemical composition of both types of bulky wastes. Qualitatively, all spectra show relatively similar appearance, but the magnitudes of particular absorption bands differ significantly. With the increasing loading of MDF wastes, the magnitude of a broad peak in the 3100–3600 cm^{-1} (stretching vibrations of O—H and N—H bonds) range was noticeably increasing, which can be attributed to the chemical structure of wood-based particles included in MDF. They are typically rich in hydroxyls, and the related signal is usually stronger than for N—H bonds in PU materials (Fornasieri et al., 2011). On the other hand, the magnitude of the signal at 1090 cm^{-1}, characteristic of the vibrations of C═O bonds in urethane groups, was gradually decreasing along with the 1512 and 1533 cm^{-1} Amide II bands, confirming a decrease in the content of PU within the analyzed composites (Mishra et al., 2012).

Considering the content and composition of the binder, hardly any differences have been observed between the particular spectra, which can be associated with the structural similarities between the generated urethanes, ureas, allophanates, and biurets, yielding very similar spectra, which can be confirmed by the similar intensity of 1090 cm^{-1} band. More noticeable differences have been observed between spectra plotted for composites obtained with varying compression molding parameters. The influence of the molding temperature and time on the magnitude of the aforementioned spectra characteristic for urethane and urea moieties was particularly noticed. Fig. 3d confirms the assumptions made based on the visual observations that the temperatures of 120 and 140 °C yielded insufficient bonding of composites' components. Simultaneously, a gradual increase of the O—H stretching band for 200 °C points to the excessive decomposition of urethane bonds. Similar observations, but to a lower extent, could be made for the influence of molding time; application of 5 and 10 min resulted in similar FTIR spectra, but the elongation of processing to 15 min unfavorably increased the extent of urethane decomposition. Notably, the decomposition and resulting stickiness of the material could be beneficial for the potential applications of prepared materials in complex structures, e.g., sandwiches, where it could strengthen interlayer bonding.

All of the samples also showed a characteristic signal around 1410 cm^{-1}, which is associated with the C–N stretching vibrations in the isocyanurate ring, the product of isocyanate trimerization (Reignier et al., 2021), which could occur between MDI binder particles. It can be distinguished from more pronounced for the analyzed material's band around 1530–1540 cm^{-1}, attributed to the C—N stretching vibrations of urethane groups. Following the work of Reignier et al. (2021), we have presented in Fig. 3 g the ratio between absorbance at 1410 cm^{-1} and 1595 cm^{-1} (phenyl C═C stretching band), which can be used to show the impact of the material's formulation on the isocyanurate generation. Obtained values below unity align with the work of Reignier et al. (2021), who obtained similar values (although slightly above unity) for PUFs obtained using isocyanate index above 1. Lower values shown for prepared materials may result from the consumption of free isocyanate groups by the functional groups of MDF waste and ammonia generated *in situ* during processing. Moreover, trimerization is typically conducted using basic catalysts like potassium octoate (Vilar, 1998). The most significant impact on the discussed absorbance ratio was noted for varying PUF:MDF ratio, which can be clearly related to the generation of isocyanate moieties during thermal degradation of PUFs and consumption of these groups by hydroxyls present in the structure of wood particles. The isocyanurate content only slightly increased with the binder content, which suggest faster reactions with other components of prepared materials compared to trimerization. On the other hand, replacing isocyanate with AB in binder composition caused a significant decrease in the isocyanurate content, which can be attributed to the lower amount of isocyanate groups in the system and their potential consumption by generated ammonia. Similar effect was noted for the increasing molding temperature and time, which can be explained by the excessive degradation of PUFs and generation of additional functionalities potentially reacting with isocyanate groups.

3.3. Morphology of prepared composites

Fig. 4 presents the morphology of prepared composite materials captured with optical and SEM microscopy. Significant variations can be noted that correspond to the observations made from the visual assessment of samples. Irrespective of the applied formulation, all samples are characterized by noticeable porosity, which can be attributed to the initial cellular structure of PUFs, their partial decomposition, as well as to the chemical reactions of MDI with AB or residual moisture present in the raw materials, yielding carbon dioxide. Considering the potential application of developed materials in the construction or building sector, it can be considered very beneficial due to the reduced thermal conductivity (Abu-Jdayil et al., 2019; Al-Homoud, 2005).

The images of sample 1, which is comprised solely of PUF, indicate its partial decomposition during compression, expressed by the smooth areas and glare observed on the optical image. A similar phenomenon can be noted for sample 2, where PUF acted as a matrix for MDF particles, which are not only deposited on the PUF phase but also embedded

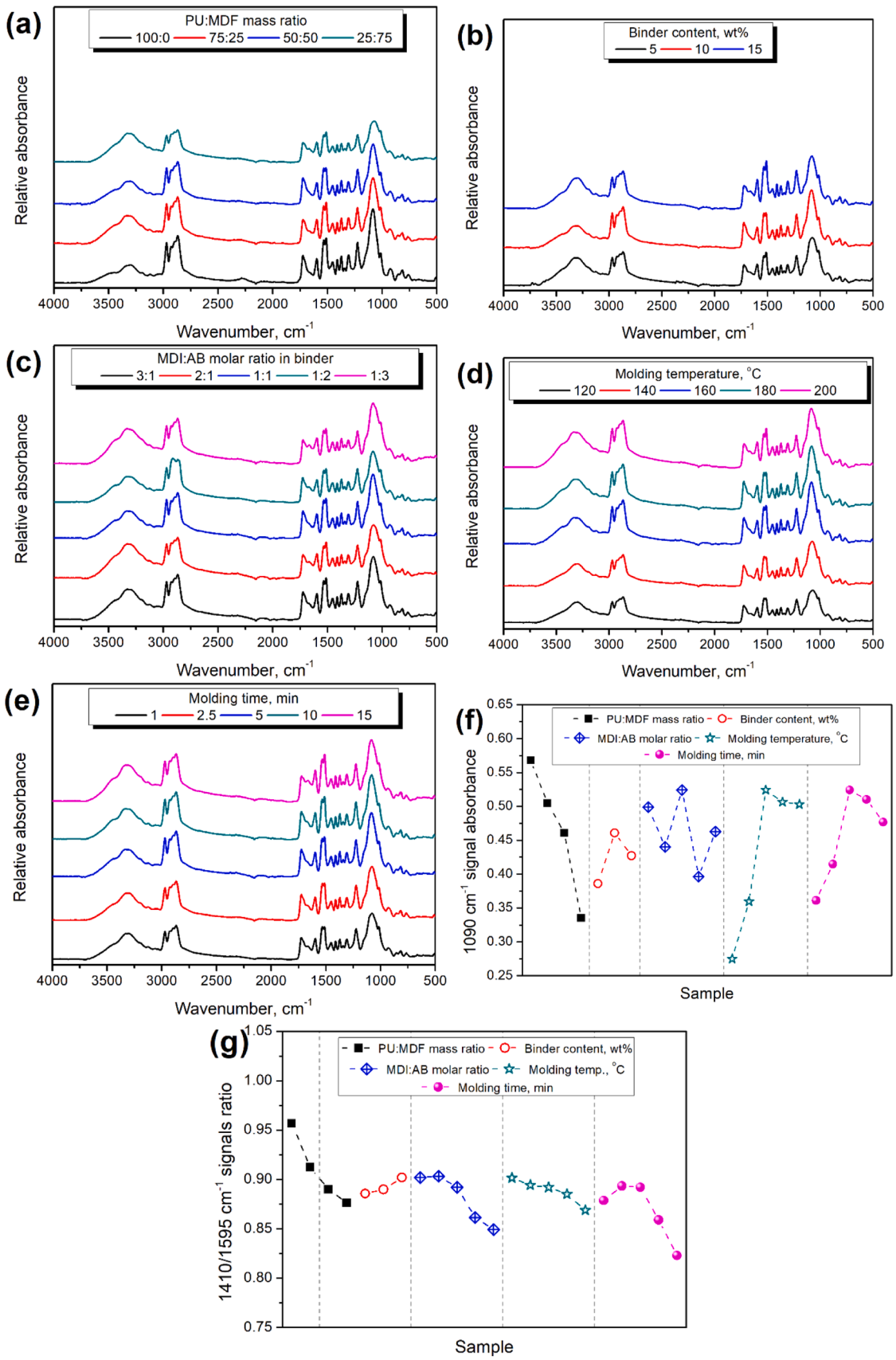

Fig. 3. The impact of (a) PUF:MDF mass ratio, (b) binder content, (c) binder composition, (d) molding temperature, and (e) molding time on the FTIR spectra plotted for prepared composites, (f) signal absorbance at 1090 cm^1, and (g) 1410/1595 cm^{-1} signals absorbance ratio.

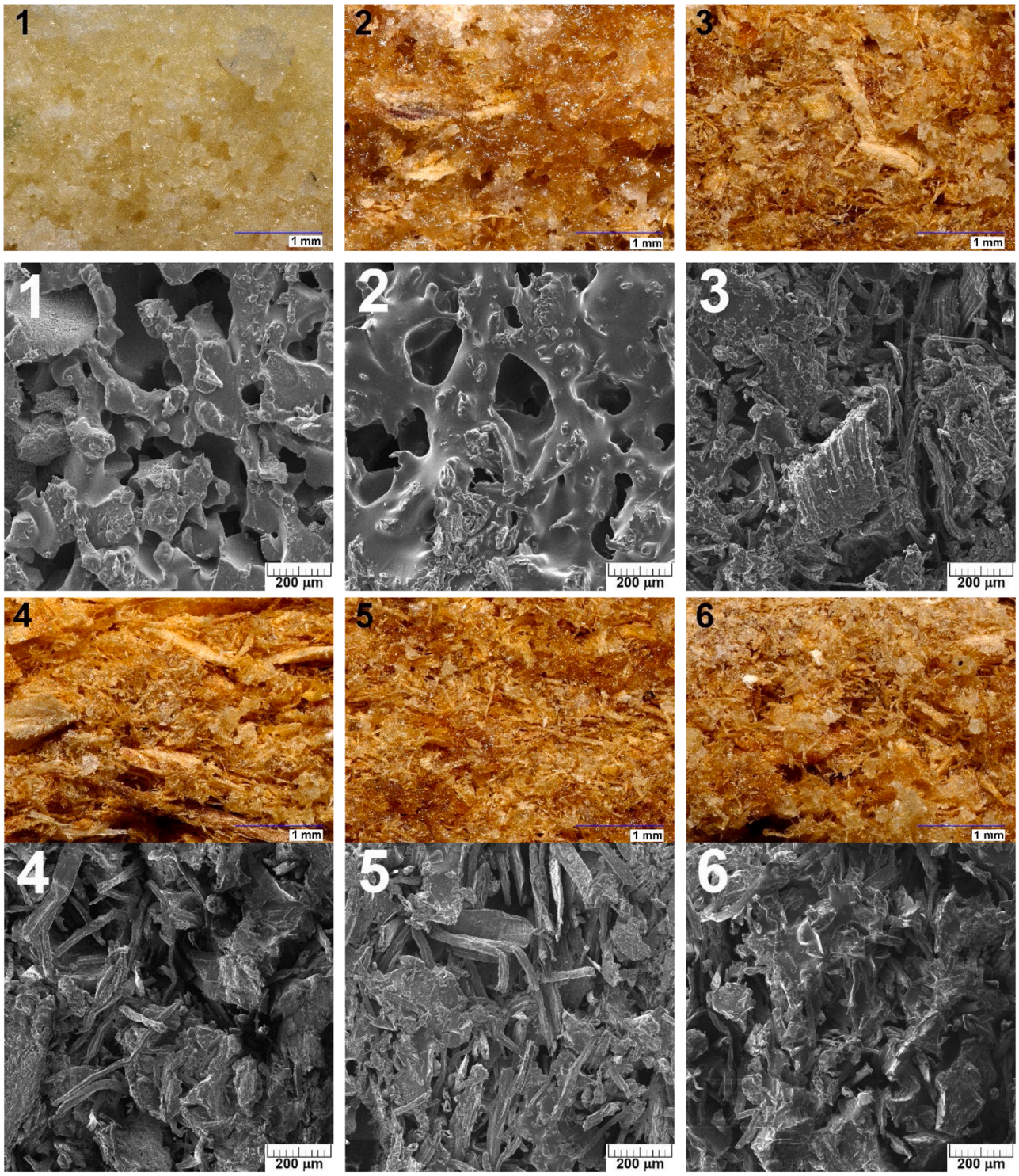

Fig. 4. Images of prepared composites' morphology obtained with optical and SEM microscopy.

into it. It suggests that elevated temperature and shear forces during compression molding caused partial decomposition and flow of the PUF phase. Moreover, good adhesion between PUF and MDF particles points to the excellent efficiency of MDI as a binder. These effects, but less pronounced due to lower PUF content, were also noted for samples 3 and 4. Nevertheless, the morphology of sample 4 confirmed visual observations related to the excessive MDF loading, which caused agglomeration of MDF particles, lately affecting mechanical performance.

Considering the impact of MDI content (samples 3, 5, and 6), only minor differences in morphology can be noted. Higher binder loading yielded increased porosity, which can be associated with slightly enhanced CO_2 generation but mainly with the lower shares of solid PUF and MDF particles. These images also point to the presence of rough structures resulting from the diisocyanate deposition on the solid particles, which have also been noted in our previous works on the surface modification of cellulose fillers (Hejna et al., 2021b; 2021a). The

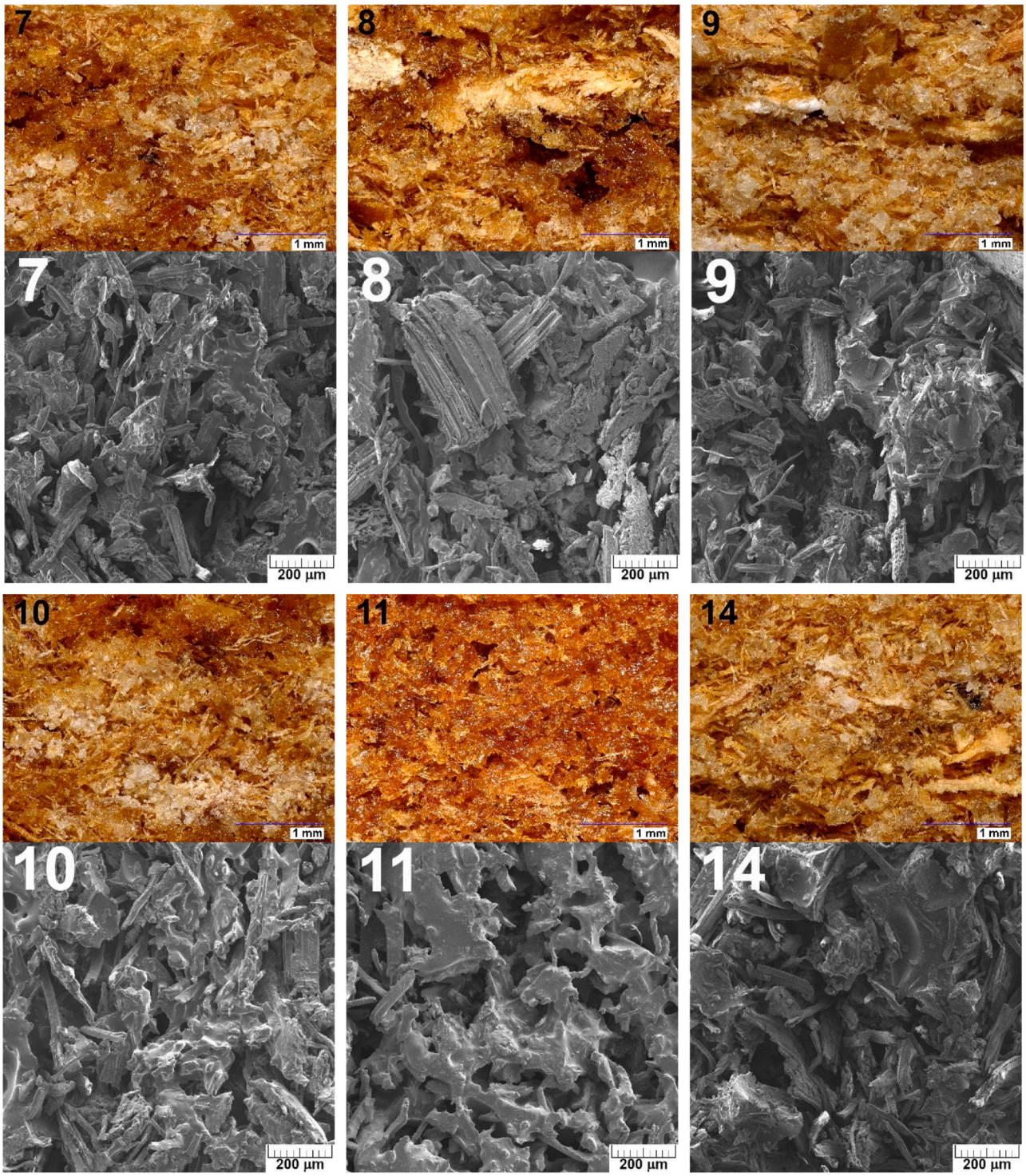

Fig. 4. (*continued*).

introduction of AB as a co-binder for MDI (samples 7–11) did not yield very significant changes when an equivalent or molar excess of MDI was applied (samples 7–9). However, when AB was introduced in excess to MDI (samples 10 and 11) and the ammonia was not entirely consumed by isocyanate groups, it caused a noticeable decomposition of PUF and its flow, enabling the encapsulation of MDF particles, observable by creating additional coating on the surface of rigid solid particles.

Increasing molding temperature (samples 9, 14, and 15), as well as elongation of molding time (samples 16, 17, 9, 18, and 19), provided relatively similar effects associated with the decomposition of PUF phase, its partial flow and covering the surface of MDF particles. However, despite the similar visual appearance and efficient encapsulation of MDF particles indicated by optical images, sample 15 showed a slightly different morphology than samples 11 and 19, which may point to the lower extent of PUF phase decomposition.

3.4. Thermal conductivity of prepared composites

The aforementioned variations in composites' structure and porosity affected their thermal insulation performance expressed by the λ

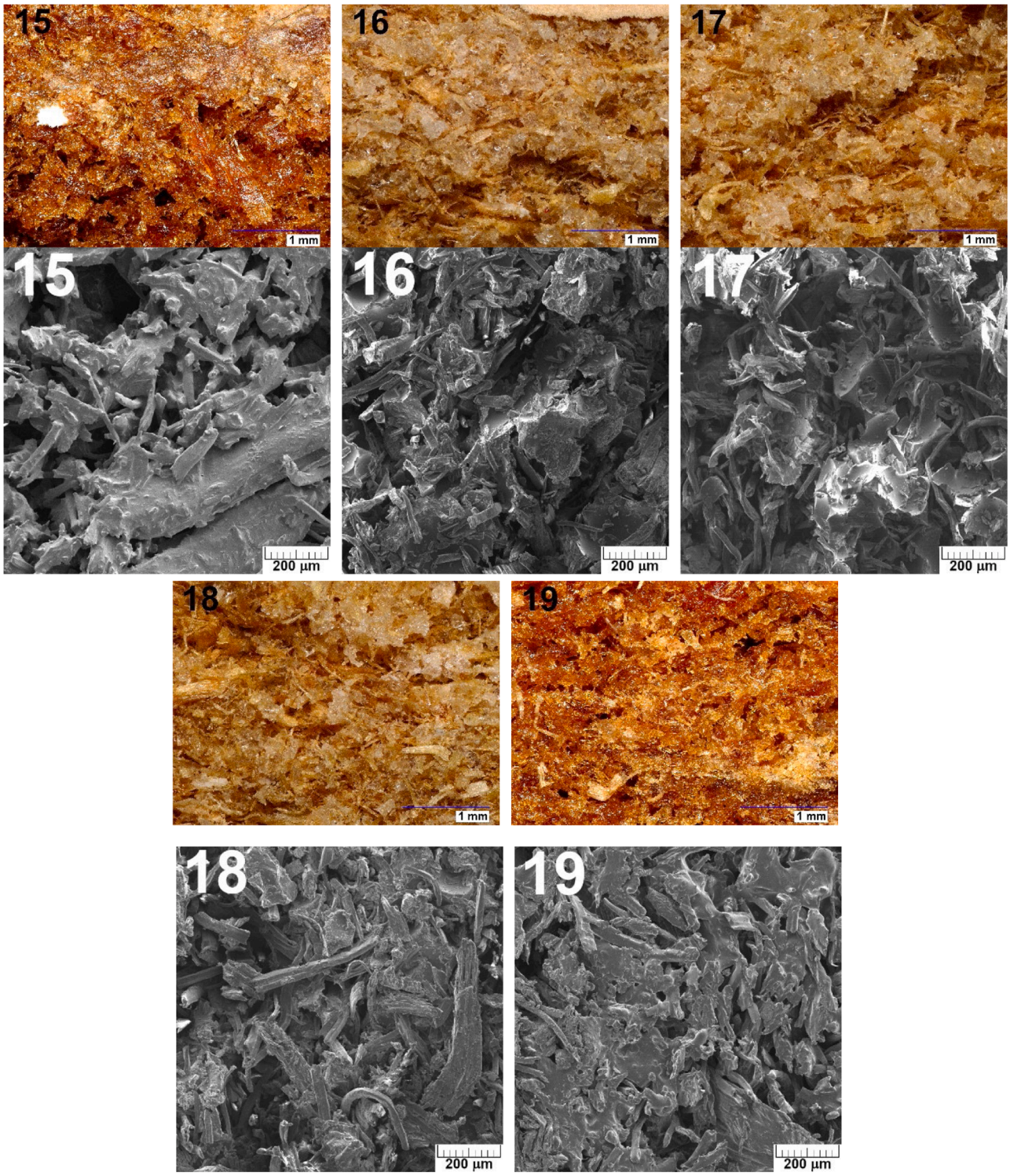

Fig. 4. (*continued*).

coefficient. Considering the potential application of prepared materials as floor underlays, the temperature range has been adjusted to mirror the actual conditions, i.e., the indoor temperature of 20 °C and the water temperature in the underfloor heating system varying from 35 to 50 °C.

Fig. 5 indicates that the λ coefficient increased with the MDF content in prepared composites, which can be associated with the excellent insulation performance of PUFs (Abu-Jdayil et al., 2022; Srihanum et al., 2022). Despite that, flexible PUFs are not applied as thermal insulation, and their λ coefficient is in the range of 60–70 mW/(m·K) (Olszewski et al., 2022a, 2022b), which is noticeably higher than ~20–25 mW/(m·K) typically noted for rigid PUFs (Andersons et al., 2020; Uram et al., 2021), they can be considered by far better insulation material than MDF with λ coefficient in the range of 100–200 mW/(m·K) (Saeed et al., 2022; Šálek et al., 2024; Taghiyari et al., 2013).

The impact of binder content and composition was not straightforward and can be associated with the changes in composites' morphology, depicted in Fig. 4. The porosity of the material implicates the presence of gas inside its structure, which typically enhances

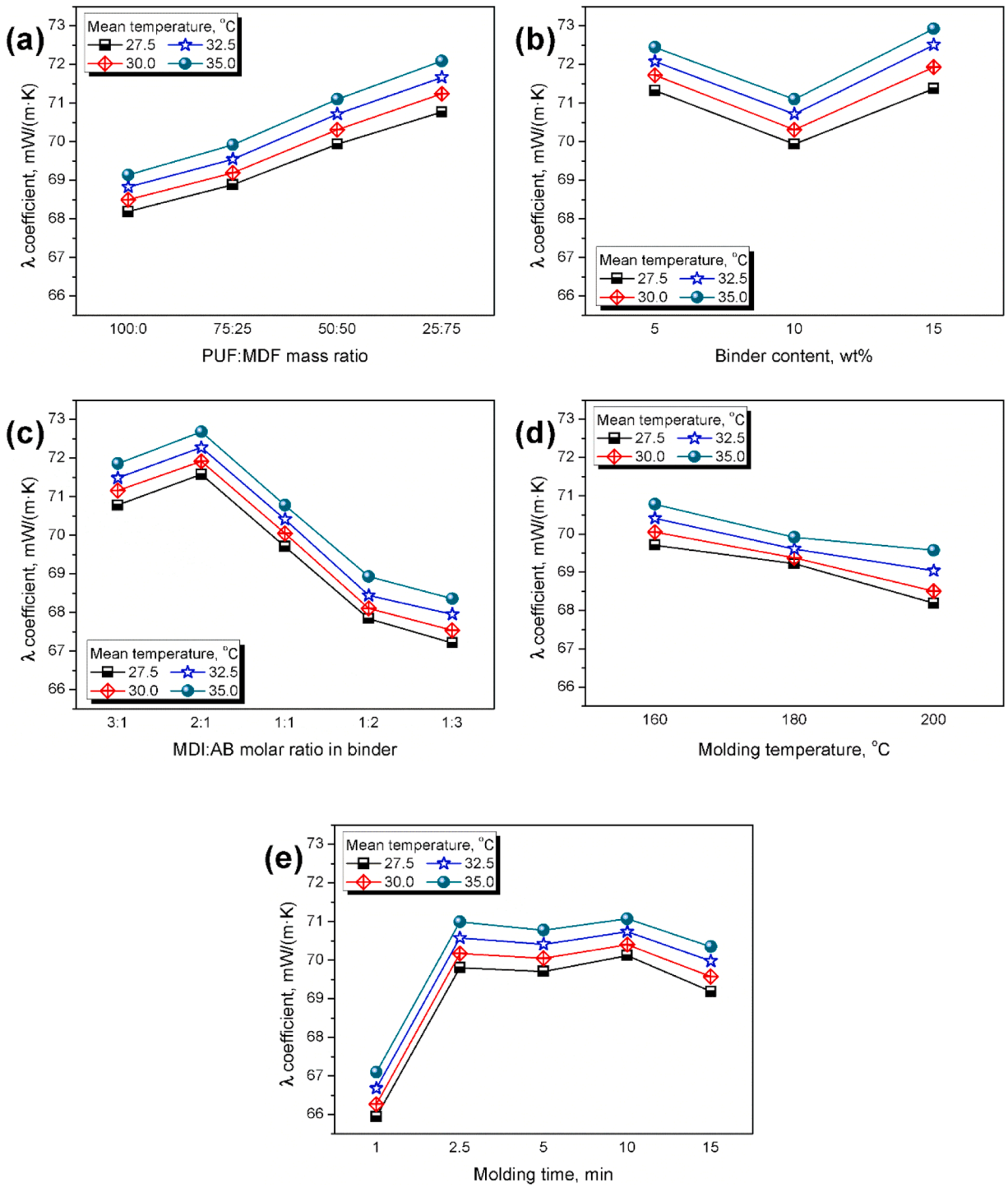

Fig. 5. The impact of (a) PUF:MDF mass ratio, (b) binder content, (c) binder composition, (d) molding temperature, and (e) molding time on thermal conductivity coefficient values of prepared composites.

insulation performance due to relatively low λ coefficients of air or carbon dioxide, around 25 and 15 mW/(m·K), respectively (Mukhopadhyaya et al., 2008). For 10 wt% binder content, the porosity was optimal, enabling efficient trapping of the gas inside the composites' structure. However, a more significant impact was noted on binder composition, which can be associated with the chemical interactions induced by AB presence and thermal decomposition of the substrates. As indicated by the TGA analysis, the whole mass of AB was converted into gas during its decomposition, which is even partially retained in the structure and enhances insulation performance. Moreover, the basic character of AB enhanced the thermal decomposition of PUF and induced its flow during compression molding, facilitating the trapping of generated gases. According to the stoichiometry, the shift of binder composition from 3:1 to 1:3 MDI:AB ratio increased the generated gases over 5 times.

The parameters of the compression molding process showed only a minor impact on thermal insulation performance. Considering temperature, its increase enhanced PUF decomposition and facilitated retaining gas inside the composite, similar to the increasing AB content in a binder. The more significant effects were noted only for the shortest

molding time of 1 min, which was attributed to the inefficient compression of material and its high porosity (see Fig. 4, sample 16). The elongation of compression time did not yield significant changes until 15 min, which, similar to the highest temperature, resulted in excessive PUF decomposition.

3.5. Mechanical performance of prepared composites

Table 2 provides details on the mechanical performance of prepared composites. Because samples 1 and 2 had very limited stiffness, measuring flexural strength due to technical aspects was impossible; therefore, only hardness values were provided. For the limited content of MDF, the hardness was noticeably lower than for the rest of the samples, confirming the results of the visual assessment of composites. On the other hand, increasing MDF content from 45 to 67.5 % (samples 3 and 4) yielded significant enhancement of the mechanical performance, owing to the increased stiffness of the material.

Considering the binder content and composition, the results also align with visual assessment and microstructure analysis. Application of 5 wt% of MDI significantly limited the strength of the material, while for 15 wt%, only a minor increase was noted compared to the 10 wt% applied for sample 3. Keeping in mind the impact mentioned above on insulation performance, as well as the environmental issues and concerns related to the application of diisocyanates (Huuskonen et al., 2023; Rother and Schlüter, 2021; Spence and Plehiers, 2022), the 10 wt % content of the binder should be considered optimal for developed materials. The incorporation of AB into binder composition and increasing its content yielded deterioration of the mechanical performance in terms of flexural strength and hardness, confirming partial decomposition of the PUF phase, related primarily to the hard segments, which comprise urethane bonds and related crosslinks (Kojio et al., 2020).

Increasing compression molding temperature resulted in the reduction of hardness, as PUF phase decomposition was noticeably enhanced (see Fig. 4, samples 9, 14, and 15). However, based on the hardness values, the extent of decomposition was lower than for the MDI:AB ratio of 1:3 (sample 11) and for the compression molding time of 15 min (sample 19), despite a similar visual appearance. It can suggest that the effect of the MDF particles' saturation by binder was higher, probably due to the higher temperature and better flowability of the decomposed PUF phase (Zia et al., 2007). At the same time, an increase in flexural strength and a noticeable reduction of deformation at flexural strength may indicate that the highest portion of PUF mechanical strength was retained or additional crosslinking occurred.

Considering the processing time, applying the shortest (1 min) and the longest (15 min) times yielded relatively weak samples, but for different reasons, the significant differences can be expressed in hardness variation. For sample 16, the processing time was insufficient to enable efficient decomposition of the PUF phase and binding MDF particles, as suggested by appearance and morphology analysis. At the same time, elongating processing caused excessive decomposition of PUF particles, which, except for the flexural strength, reduced the material's hardness.

Table 2
The mechanical parameters of prepared composites.

Sample	Flexural strength, kPa	Deformation at flexural strength, %	Hardness, Sh0
1	–	–	51.3 ± 3.3
2	–	–	57.9 ± 4.5
3	204.7 ± 60.5	5.6 ± 1.1	76.8 ± 3.1
4	348.3 ± 71.6	1.6 ± 0.7	89.9 ± 3.8
5	61.9 ± 50.2	6.9 ± 1.7	72.1 ± 3.4
6	239.3 ± 47.6	3.9 ± 0.9	83.6 ± 4.0
7	232.7 ± 64.3	5.6 ± 0.7	81.7 ± 3.1
8	167.3 ± 14.6	5.5 ± 0.9	78.8 ± 3.9
9	153.7 ± 10.8	5.7 ± 1.1	75.1 ± 3.2
10	147.0 ± 4.5	5.4 ± 0.3	66.6 ± 3.3
11	95.1 ± 11.9	6.3 ± 1.9	62.7 ± 3.0
14	167.7 ± 11.1	5.1 ± 0.7	73.2 ± 2.9
15	195.0 ± 5.7	2.5 ± 0.7	67.2 ± 3.6
16	75.1 ± 6.3	5.5 ± 0.5	74.2 ± 4.0
17	164.5 ± 3.7	5.6 ± 1.5	76.2 ± 2.5
18	120.2 ± 4.3	6.9 ± 1.2	76.4 ± 2.7
19	77.7 ± 13.2	6.2 ± 1.3	65.2 ± 4.6

3.6. Thermal stability of prepared composites

Fig. 6 presents the mass loss curves and differential curves (DTG) obtained during the TGA of prepared composites. Similar to the other aspects, the most significant impact was noted for the mass ratio between PUF and MDF wastes, which originated from the different natures of these materials. Increasing MDF loading significantly increased the content of char residue from 7.9 wt% for sample 1 to 20.4 wt% for sample 4, pointing to the carbonization of the plant-based components present in wood particles. Simultaneously, the onset of thermal decomposition, expressed as the temperature corresponding to the 2 wt % mass loss, was shifted from 242.9 °C to 209.0 °C, which may be associated with the moisture absorption of hydrophilic wood particles (Pouzet et al., 2015). Such a phenomenon can be confirmed by the appearance of additional signals on DTG curves around 60–65 °C. Such a signal was not observed for sample 1, comprising solely of PUF waste. At the same time, the course of thermal decomposition significantly differed. PUFs are typically composed of hard and soft segments. Despite the low content of the first group in flexible PUFs, the corresponding decomposition step is typically noted during TGA (Kosmela et al., 2021b; 2021a). In the presented case, it can be expressed by a minor signal of around 250 °C. For samples containing MDF wastes, the separate signal was not noted due to the overlapping with other signals. Considering the soft segments, their decomposition occurs at higher temperatures, and the decrease of the peak slightly above 400 °C can be noted with the increasing MDF loading.

Variations in the binder's content hardly affected the composites' thermal stability and degradation course. The decomposition onset was slightly shifted toward higher temperatures, from 219.2 °C to 227.2 °C, which can be associated with enhanced structure crosslinking and reduced diffusion of less stable components. A more notable impact was noted for the binder's composition. For sample 3, which contained only MDI, the degradation onset was 222.5 °C. Introduction of AB (sample 7, 3:1 MDI:AB ratio) reduced it to 219.5 °C, while equal MDI and AB contents (sample 9, 1:1 MDI:AB ratio), and the excess of AB (sample 11, 1:3 MDI:AB ratio) yielded values of 213.4 °C and 171.7 °C, respectively. Such a significant reduction of stability confirms an excessive decomposition of the PUF phase. It noticeably facilitates the release of less stable components, confirmed by the magnitude of the corresponding peak on the DTG curve.

Increasing the temperature applied during compression molding hardly affected the thermal stability and decomposition of composites. These changes confirm the conclusions drawn from the mechanical tests and point to limited PUF degradation compared to high AB loading despite samples' similar appearance and morphology. Similarly, elongating the compression molding process to 15 min caused excessive degradation, which reduced thermal decomposition onset from 220.0 °C for 10 min to 208.1 °C, which points to the facilitated release of particular components of prepared composites.

Nevertheless, all of the analyzed materials except sample 11 showed satisfactory thermal stability exceeding 200 °C, which should be sufficient for their industrial applications. Moreover, additional treatments aimed at reducing moisture absorption should further enhance the stability.

3.7. Acoustic performance of prepared composites

Based on the results mentioned above, mainly the morphology and

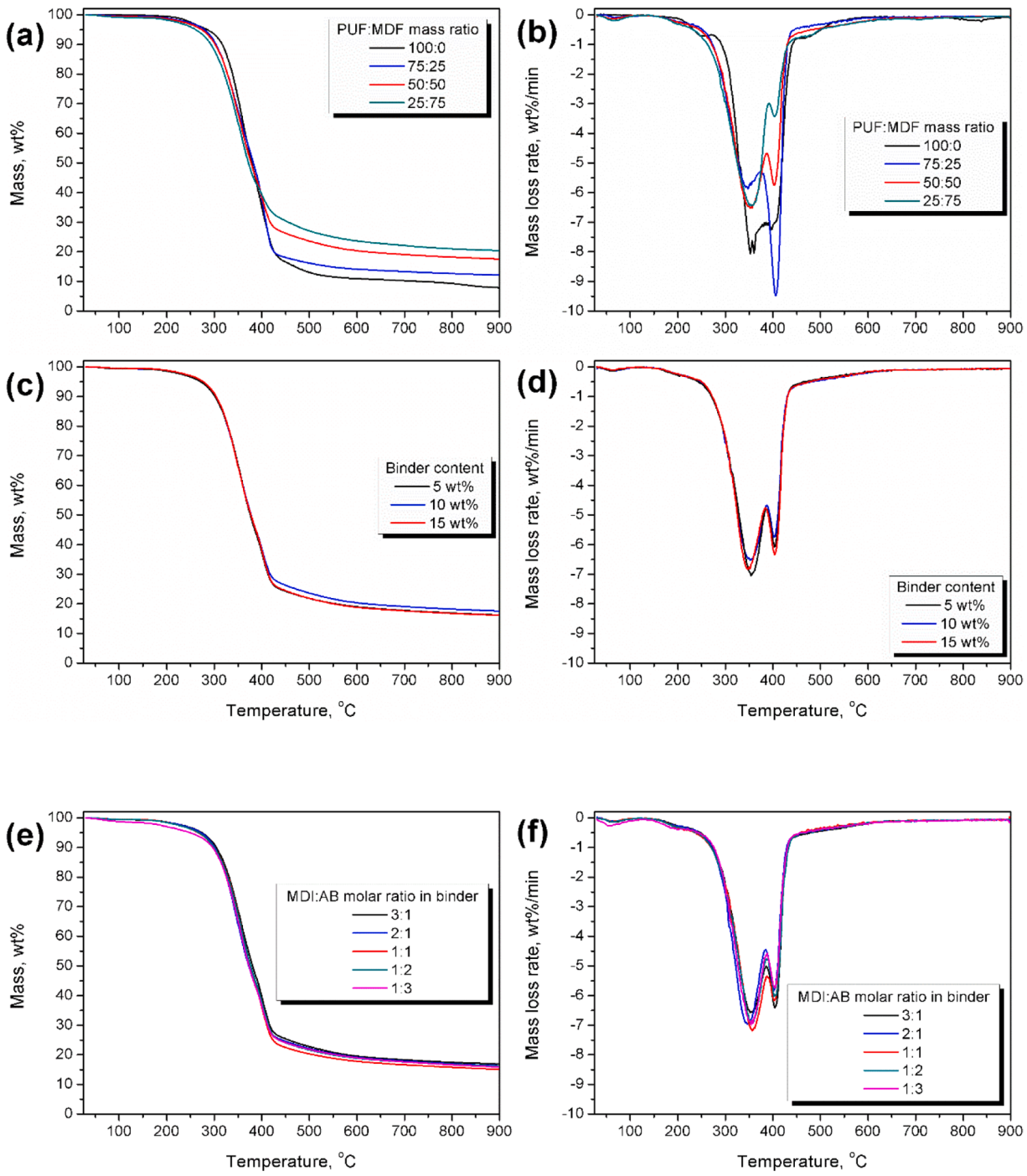

Fig. 6. The impact of (a,b) PUF:MDF mass ratio, (c,d) binder content, (e,f) binder composition, (g,h) molding temperature, and (i,j) molding time on thermal degradation of prepared composites.

thermal insulation properties of prepared composites, selected samples have been investigated in terms of their acoustic performance. Sample 3, composed of PU and MDF in 50:50 ratio containing solely MDI as a binder, was analyzed along with samples 7, 9, and 11 containing MDI: AB combination, respectively, in 3:1, 1:1, and 1:3 ratios. Fig. 7 presents plots of sound absorption coefficient characteristics of selected composite samples in 1/3 octave bands (100–6300 Hz).

Considering the impact of morphology, materials predisposed to good sound attenuation should be characterized by high porosity and open-cell structure (Abdollahi Baghban et al., 2018). Micro deformations inside the material induced by the conversion of sound energy into heat are significantly facilitated by increasing pore size and interconnected porosity (Zhang et al., 2012). For all of the analyzed materials, the sound absorption coefficient increased with sound frequency, which is a typical effect for porous materials due to the decreasing wavelength, which facilitates the penetration of structure by sound waves (Małysa et al., 2016).

In the presented case, all the analyzed materials show relatively similar sound attenuation performance despite the noticeable differences in thermal insulation performance, which is also structure-dependent. Apparently, the introduction of AB increased gas generation. Due to the enhanced PU phase, decomposition was efficiently

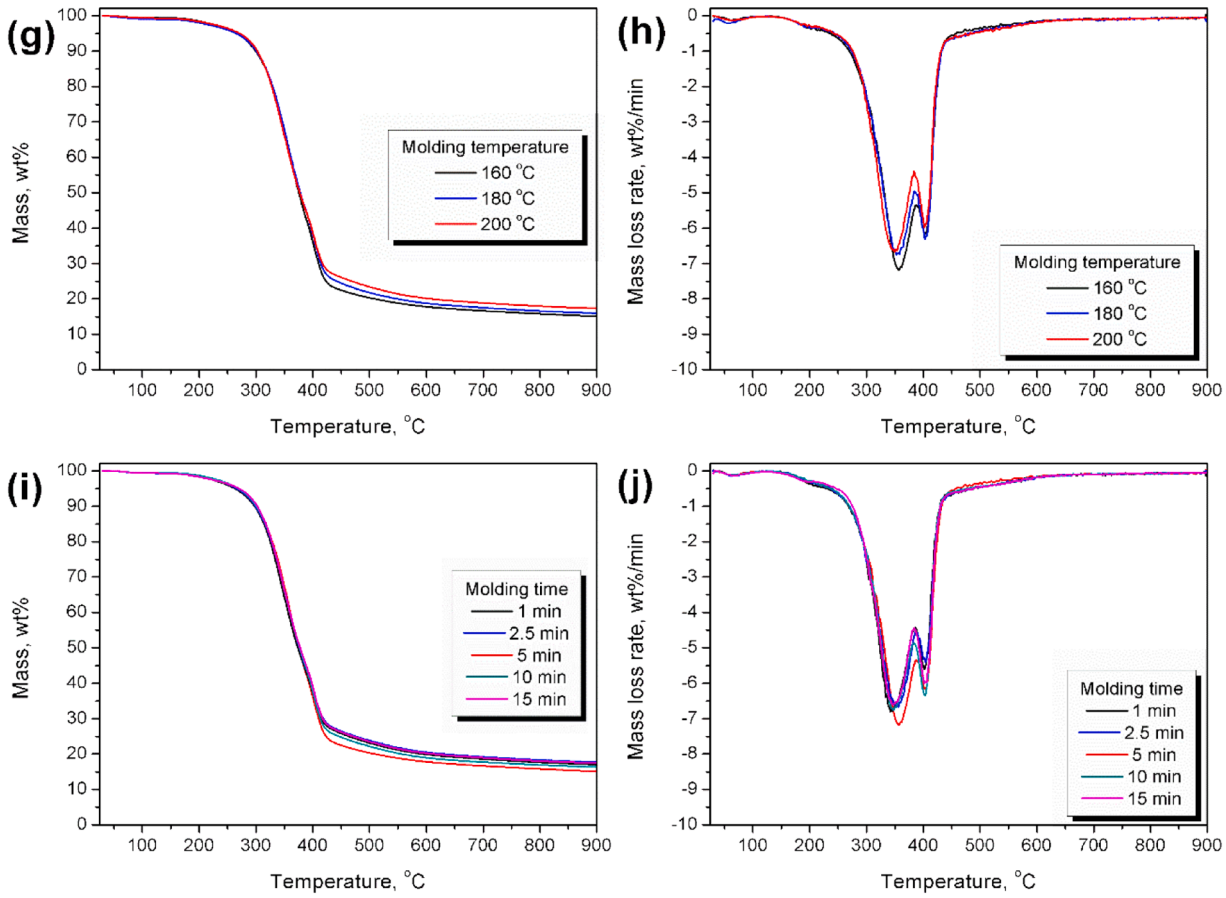

Fig. 6. (*continued*).

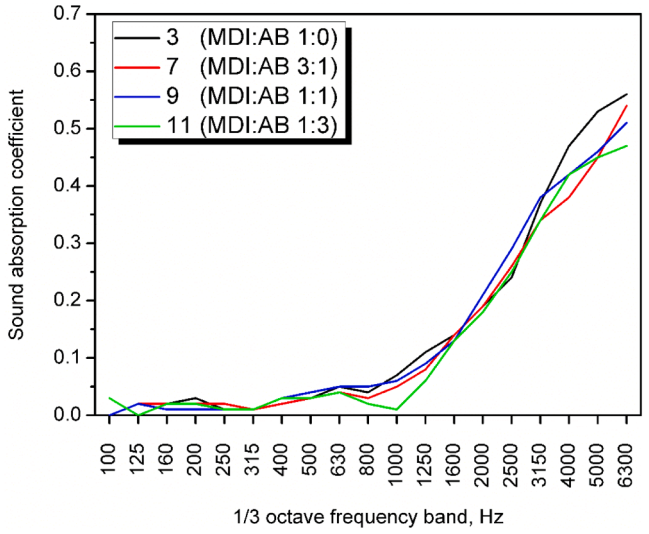

Fig. 7. Sound absorption coefficients of selected composite samples in 1/3 octave bands (100–6300 Hz).

trapped inside the structure, which showed hardly any impact on sound absorption. This may be related to two phenomena (i) the formation of closed pores not actively participating in sound absorption due to Helmholtz resonance, or (ii) the limitation of the specific surface area of the rigid MDF particles that actively participated in the propagation of the sound wave. Nevertheless, the presented results indicate that all of the analyzed materials could be applied as auxiliaries for sound attenuation above 4 kHz.

4. Conclusions

The presented work provided auspicious insights into the application of two types of commonly generated bulky wastes: flexible PUFs used as mattresses and MDFs used in furniture products as raw materials for novel composites with potential applications in the construction and building sector. They have been manufactured using a common and relatively simple process of compression molding, with the addition of an innovative binder composed of widely applied methylene diphenyl diisocyanate and ammonium bicarbonate. Such a simple change in the binder composition resulted in a multitude of additional chemical interactions leading to the decomposition of PUF materials, enhanced gas generation, and additional crosslinking strengthening the interfacial adhesion. The impact of these reactions on the appearance, morphology, mechanical, thermal, and insulation performance of prepared composites has been evaluated. Prepared samples showed the highest flexural strength of 348.3 kPa and hardness of 89.9 Sh0 for the PUF:MDF ratio of 25:75, while for the equal shares of both wastes (selected for further analyses), the most beneficial parameters, tensile strength of 239.3 kPa and hardness of 83.6 Sh0 were noted when 15 wt% of MDI was applied as binder. Replacing MDI with AB yielded reduction of the mechanical parameters, which was, however, balanced by the insulation performance, expressed by the 5 % decrease in thermal conductivity coefficient. The obtained results pointed to the optimal formulations for developed composites, providing an adequate extent of PUF decomposition, which yielded efficient encapsulation of MDF particles and retaining generated gases inside the structure, as indicated by the morphology observations. However, despite the adverse impact of excessive PUF degradation noted in the presented work, it can be

considered a very promising direction for developing novel, waste-based binders for engineered wood materials. Concluding, presented results indicate that by the adjustment of binder composition, the performance of developed materials can be adjusted to find a proper balance between the mechanical performance and insulation properties for the particular products, e.g., to replace fiberboard in less demanding applications like masking or finishing materials.

CRediT authorship contribution statement

Aleksander Hejna: Writing – review & editing, Writing – original draft, Visualization, Validation, Supervision, Resources, Project administration, Methodology, Investigation, Funding acquisition, Formal analysis, Data curation, Conceptualization. **Mateusz Barczewski:** Writing – review & editing, Funding acquisition, Formal analysis. **Joanna Aniśko:** Investigation. **Adam Piasecki:** Visualization, Methodology, Investigation. **Roman Barczewski:** Writing – review & editing, Methodology, Investigation, Formal analysis. **Paulina Kosmela:** Methodology, Investigation. **Jacek Andrzejewski:** Writing – review & editing, Formal analysis. **Marek Szostak:** Formal analysis.

Declaration of competing interest

The authors declare that they have no known competing financial interests or personal relationships that could have appeared to influence the work reported in this paper.

Acknowledgments

This work was subsidized from the state budget of Poland under the Ministry of Education and Science programme "Science for the Society II" project "INNOGOW—Supporting innovation in bulky waste management," project number NdS-II/SP/0039/2024/01, funding amount PLN 1,063,700.00, total project value PLN 1,063,700.00. Moreover, the work was supported by the Ministry of Science and Higher Education in Poland (grant number 0612/SBAD/3605).

Supplementary materials

Supplementary material associated with this article can be found, in the online version, at doi:10.1016/j.rcradv.2025.200244.

Data availability

Data will be made available on request.

References

Abdollahi Baghban, S., Khorasani, M., Sadeghi, G.M.M., 2018. Soundproofing flexible polyurethane foams: the impact of polyester chemical structure on the microphase separation and acoustic damping. J. Appl. Polym. Sci. 135, 46744. https://doi.org/10.1002/app.46744.

Abu-Jdayil, B., Al Abdallah, H., Mlhem, A., Alkhatib, S., El Sayah, A., Hussein, H., Althabahi, A., AlAydaroos, A., 2022. Utilization of polyurethane foam dust in development of thermal insulation composite. Buildings 12, 126. https://doi.org/10.3390/buildings12020126.

Abu-Jdayil, B., Mourad, A.-H., Hittini, W., Hassan, M., Hameedi, S., 2019. Traditional, state-of-the-art and renewable thermal building insulation materials: an overview. Constr. Build. Mater. 214, 709–735. https://doi.org/10.1016/j.conbuildmat.2019.04.102.

Al-Homoud, Dr.M.S., 2005. Performance characteristics and practical applications of common building thermal insulation materials. Build. Environ. 40, 353–366. https://doi.org/10.1016/j.buildenv.2004.05.013.

Allan, D., Daly, J.H., Liggat, J.J., 2019. Oxidative and non-oxidative degradation of a TDI-based polyurethane foam: volatile product and condensed phase characterisation by FTIR and solid state 13C NMR spectroscopy. Polym. Degrad. Stab. 161, 57–73. https://doi.org/10.1016/j.polymdegradstab.2018.12.027.

Andersons, J., Kirpluks, M., Cabulis, P., Kalnins, K., Cabulis, U., 2020. Bio-based rigid high-density polyurethane foams as a structural thermal break material. Constr. Build. Mater. 260, 120471. https://doi.org/10.1016/j.conbuildmat.2020.120471.

Bohringer, C., 2003. The Kyoto protocol: a review and perspectives. Oxf. Rev. Econ. Policy. 19, 451–466. https://doi.org/10.1093/oxrep/19.3.451.

Boruszewski, P., Borysiuk, P., Jankowska, A., Pazik, J., 2022. Low-density particleboards modified with expanded and unexpanded fillers—characteristics and properties. Materials (Basel) 15, 4430. https://doi.org/10.3390/ma15134430.

de Melo, T.A.C., de Oliveira, M.A., de Sousa, S.R.G., Vieira, R.K., Amaral, T.S., 2022. Circular economy public policies: a systematic literature review. Procedia Comput. Sci. 204, 652–662. https://doi.org/10.1016/j.procs.2022.08.079.

Ding, Y., Pang, Z., Lan, K., Yao, Y., Panzarasa, G., Xu, L., Lo Ricco, M., Rammer, D.R., Zhu, J.Y., Hu, M., Pan, X., Li, T., Burgert, I., Hu, L., 2023. Emerging engineered wood for building applications. Chem. Rev. 123, 1843–1888. https://doi.org/10.1021/acs.chemrev.2c00450.

European Comission, 2020a. Communication From The Commission To The European Parliament, The Council, The European Economic And Social Committee of the Regions. A new Circular Economy Action Plan For a cleaner and more competitive Europe. https://eur-lex.europa.eu/legal-content/EN/TXT/?qid=1583933814386&uri=COM:2020:98:FIN.

European Comission, 2020b. State of the Union: commission raises climate ambition and proposes 55% cut in emissions by 2030. https://ec.europa.eu/commission/presscorner/detail/en/ip_20_1599.

European Comission, 2019. The European Green Deal sets out how to make Europe the first climate-neutral continent by 2050, boosting the economy, improving people's health and quality of life, caring for nature, and leaving no one behind. https://ec.europa.eu/commission/presscorner/detail/en/ip_19_6691.

European Environment Agency, 2023. Reaching 2030's residual municipal waste target — Why recycling is not enough [WWW Document]. https://www.eea.europa.eu/publications/reaching-2030s-residual-municipal-waste.

Fornasieri, M., Alves, J.W., Muniz, E.C., Ruvolo-Filho, A., Otaguro, H., Rubira, A.F., Carvalho, G.M.de, 2011. Synthesis and characterization of polyurethane composites of wood waste and polyols from chemically recycled pet. Compos. Part a Appl. Sci. Manuf. 42, 189–195. https://doi.org/10.1016/j.compositesa.2010.11.004.

Glowny Urzad Statystyczny. Ochrona środowiska 2023 [WWW Document] https://stat.gov.pl/download/gfx/portalinformacyjny/pl/defaultaktualnosci/5484/1/24/1/ochrona_srodowiska_2023.pdf.

Gu, X., Wang, X., Guo, X., Liu, S., Lou, C., Liu, Y., 2023. Study on efficient degradation of Waste PU foam. Polymers. (Basel) 15, 2359. https://doi.org/10.3390/polym15102359.

Hejna, A., Barczewski, M., 2024. Sposób wytwarzania kształtek z wykorzystaniem odpadów pianki poliuretanowej. P.448539.

Hejna, A., Marć, M., Korol, J., 2021a. Modification of cellulosic filler with diisocyanates – volatile organic compounds emission assessment and stability of chemical structure over time. Nord. Pulp. Paper. Res. J. 36, 353–372. https://doi.org/10.1515/npprj-2020-0104.

Hejna, A., Marć, M., Skórczewska, K., Szulc, J., Korol, J., Formela, K., 2021b. Insights into modification of lignocellulosic fillers with isophorone diisocyanate: structure, thermal stability and volatile organic compounds emission assessment. Eur. J. Wood Wood Prod. 79, 75–90. https://doi.org/10.1007/s00107-020-01604-y.

Huuskonen, P., Porras, S.P., Scholten, B., Portengen, L., Uuksulainen, S., Ylinen, K., Santonen, T., 2023. Occupational exposure and health impact assessment of diisocyanates in Finland. Toxics. 11, 229. https://doi.org/10.3390/toxics11030229.

Hýsek, Š., Neuberger, P., Sikora, A., Schönfelder, O., Ditommaso, G., 2019. Waste utilization: insulation panel from recycled polyurethane particles and wheat husks. Materials (Basel) 12, 3075. https://doi.org/10.3390/ma12193075.

Khatoon, H., Iqbal, S., Irfan, M., Darda, A., Rawat, N.K., 2021. A review on the production, properties and applications of non-isocyanate polyurethane: a greener perspective. Prog. Org. Coat. 154, 106124. https://doi.org/10.1016/j.porgcoat.2020.106124.

Kirchherr, J., Reike, D., Hekkert, M., 2017. Conceptualizing the circular economy: an analysis of 114 definitions. Resour. Conserv. Recycl. 127, 221–232. https://doi.org/10.1016/j.resconrec.2017.09.005.

Kojio, K., Nozaki, S., Takahara, A., Yamasaki, S., 2020. Influence of chemical structure of hard segments on physical properties of polyurethane elastomers: a review. Journal of Polymer Research 27, 140. https://doi.org/10.1007/s10965-020-02090-9.

Kosmela, P., Olszewski, A., Zedler, Ł., Burger, P., Piasecki, A., Formela, K., Hejna, A., 2021a. Ground tire rubber filled flexible polyurethane foam—effect of waste rubber treatment on composite performance. Materials (Basel) 14. https://doi.org/10.3390/ma14143807.

Kosmela, P., Olszewski, A., Zedler, Ł., Hejna, A., Burger, P., Formela, K., 2021b. Structural changes and their implications in foamed flexible polyurethane composites filled with rapeseed oil-treated ground tire rubber. J. Compos. Sci. 5. https://doi.org/10.3390/jcs5030090.

Lauri, P., Kallio, A.M.I., Schneider, U.A., 2012. Price of CO2 emissions and use of wood in Europe. For. Policy. Econ. 15, 123–131. https://doi.org/10.1016/j.forpol.2011.10.003.

Levchik, S.V., Weil, E.D., 2004. Thermal decomposition, combustion and fire-retardancy of polyurethanes—a review of the recent literature. Polym. Int. 53, 1585–1610. https://doi.org/10.1002/pi.1314.

Ma, Y., Song, J., Jiang, Y., Zhang, Y., Gu, J., 2022. Preparation of isocyanate microcapsules by interfacial polymerization/in-situ polymerization and their application in wood adhesives. J. Adhes. 98, 2689–2705. https://doi.org/10.1080/00218464.2021.1988939.

Małysa, T., Nowacki, K., Wieczorek, J., 2016. Assessment of sound absorbing properties of polyurethane sandwich system. Compos. Theory Pract. 16, 244–248.

Mao, A., Shmulsky, R., Li, Q., Wan, H., 2014. Recycling polyurethane materials: a comparison of polyol from glycolysis with micronized polyurethane powder in particleboard applications. Bioresources 9, 4253–4265.

Mishra, A.K., Narayan, R., Raju, K.V.S.N., Aminabhavi, T.M., 2012. Hyperbranched polyurethane (HBPU)-urea and HBPU-imide coatings: effect of chain extender and NCO/OH ratio on their properties. Prog. Org. Coat. 74, 134–141. https://doi.org/10.1016/j.porgcoat.2011.11.027.

Mukhopadhyaya, P., Kumaran, K., Normandin, N., van Reenen, D., Lackey, J., 2008. High-performance vacuum insulation panel: development of alternative core materials. Journal of Cold Regions Engineering 22, 103–123. https://doi.org/10.1061/(ASCE)0887-381X(2008)22:4(103).

Muñoz, S., Hosseini, M.R., Crawford, R.H., 2024. Towards a holistic assessment of circular economy strategies: the 9R circularity index. Sustain. Prod. Consum. 47, 400–412. https://doi.org/10.1016/j.spc.2024.04.015.

Niesiobędzka, J., Datta, J., 2023. Challenges and recent advances in bio-based isocyanate production. Green Chem. 25, 2482–2504. https://doi.org/10.1039/D2GC04644J.

Olszewski, A., Kosmela, P., Piasecki, A., Barczewski, M., Hejna, A., 2022a. The impact of isocyanate index and filler functionalities on the performance of flexible foamed polyurethane/ground tire rubber composites. Polymers. (Basel) 14, 5558. https://doi.org/10.3390/polym14245558.

Olszewski, A., Kosmela, P., Piasecki, A., Żukowska, W., Szczepański, M., Wojtasz, P., Barczewski, M., Barczewski, R., Hejna, A., 2022b. Comprehensive investigation of stoichiometry–structure–performance relationships in flexible polyurethane foams. Polymers. (Basel) 14, 3813. https://doi.org/10.3390/polym14183813.

Payne, J., McKeown, P., Jones, M.D., 2019. A circular economy approach to plastic waste. Polym. Degrad. Stab. 165, 170–181. https://doi.org/10.1016/j.polymdegradstab.2019.05.014.

Pouzet, M., Gautier, D., Charlet, K., Dubois, M., Béakou, A., 2015. How to decrease the hydrophilicity of wood flour to process efficient composite materials. Appl. Surf. Sci. 353, 1234–1241. https://doi.org/10.1016/j.apsusc.2015.06.100.

Reignier, J., Méchin, F., Sarbu, A., 2021. Chemical gradients in PIR foams as probed by ATR-FTIR analysis and consequences on fire resistance. Polym. Test. 93, 106972. https://doi.org/10.1016/j.polymertesting.2020.106972.

Rother, D., Schlüter, U., 2021. Occupational exposure to diisocyanates in the European Union. Ann. Work Expo Health 65, 893–907. https://doi.org/10.1093/annweh/wxab021.

Saeed, N., Malen, J.A., Chamanzar, M., Krishnamurti, R., 2022. Experimental correlation of thermal conductivity with dielectric properties of wood and wood-based materials: possibilities for rapid in-situ building energy evaluation. J. Build. Eng. 50, 104178. https://doi.org/10.1016/j.jobe.2022.104178.

Šálek, V., Hasalová, L., Štejfa, V., Pivák, A., Hejtmánek, P., Ira, J., Jahoda, M., 2024. Sensitivity study of measured wooden board thermal properties on solid heat transfer model predictions. Fire Saf. J. 143, 104055. https://doi.org/10.1016/j.firesaf.2023.104055.

Spence, M.W., Plehiers, P.M., 2022. A brief overview of properties and reactions of diisocyanates. Toxicol. Ind. Health 38, 495–499. https://doi.org/10.1177/07482337221090709.

Srihanum, A., Tuan Noor, M.T., Devi, K.P., Hoong, S.S., Ain, N.H., Mohd, N.S., Nek Mat Din, N.S.M., Kian, Y.S., 2022. Low density rigid polyurethane foam incorporated with renewable polyol as sustainable thermal insulation material. J. Cell Plast. 58, 485–503. https://doi.org/10.1177/0021955×211062630.

Taghiyari, H.R., Mobini, K., Samadi, Y.S., Doosti, Z., Nouri, P., 2013. Effects of nano-wollastonite on thermal conductivity coefficient of medium-density fiberboard. J. Nanomater. Molec. Nanotechnol. 02. https://doi.org/10.4172/2324-8777.1000106.

Uram, K., Prociak, A., Vevere, L., Pomilovskis, R., Cabulis, U., Kirpluks, M., 2021. Natural oil-based rigid polyurethane foam thermal insulation applicable at cryogenic temperatures. Polymers. (Basel) 13, 4276. https://doi.org/10.3390/polym13244276.

Vilar, W.D., 1998. Química e Tecnologia dos Poliuretanos. Vilar Consultoria Técnica Ltda, Rio de Janeiro, Brazil, 2nd ed. ed.

Zhang, C., Li, J., Hu, Z., Zhu, F., Huang, Y., 2012. Correlation between the acoustic and porous cell morphology of polyurethane foam: effect of interconnected porosity. Mater. Des. 41, 319–325. https://doi.org/10.1016/j.matdes.2012.04.031.

Zhao, X., Korey, M., Li, K., Copenhaver, K., Tekinalp, H., Celik, S., Kalaitzidou, K., Ruan, R., Ragauskas, A.J., Ozcan, S., 2022. Plastic waste upcycling toward a circular economy. Chem. Eng. J. 428, 131928. https://doi.org/10.1016/j.cej.2021.131928.

Zia, K.M., Bhatti, H.N., Ahmad Bhatti, I., 2007. Methods for polyurethane and polyurethane composites, recycling and recovery: a review. React. Funct. Polym. 67, 675–692. https://doi.org/10.1016/j.reactfunctpolym.2007.05.004.